Journal of Power Sources 196 (2011) 6583–6587

Contents lists available at ScienceDirect

Journal of Power Sources

journal homepage: www.elsevier.com/locate/jpowsour

Short communication

Gas evolution in a flow-assisted zinc–nickel oxide battery

Yasumasa Ito*, Michael Nyce, Robert Plivelich, Martin Klein, Sanjoy Banerjee

CUNY Energy Institute, Department of Chemical Engineering, The City College of the City University of New York, 140th St at Convent Ave, New York, NY 10031, USA

ARTICLE INFO

Article history:
Received 24 February 2011
Received in revised form 9 March 2011
Accepted 12 March 2011
Available online 22 March 2011

Keywords:
Zinc–nickel oxide battery
Flow battery
Hydrogen evolution
Oxygen evolution
Coulombic efficiency
Electrolyte

ABSTRACT

An experimental study on hydrogen and oxygen evolution was carried out in a sealed zinc–nickel oxide battery. The effects of flowing electrolyte on gas evolution were quantitatively evaluated. The results show that both the hydrogen and oxygen evolution are suppressed by making the electrolyte flow on a regular cycle. This is due to increased cell polarization in the non-flowing case attributed to the concentration boundary layer of zinc (zincate) ion near the anode surfaces. Though the Coulombic efficiency in the flowing case was higher than that in the non-flowing case, the fraction of gas evolution against Coulombic loss was the same for both the cases. When deeply discharging the cell, more hydrogen is evolved in the flowing case than in the non-flowing case.

1. Introduction

With increasing demand of efficient use of excess night-time generation capacity and intermittent renewable sources of energy like the sun and wind, it is expected to develop economical means of electricity storage. Zinc-based rechargeable batteries are one of the most attractive electrical energy storage systems due to its advantages such as low cost, abundance, green, and higher energy density when compared with conventional batteries.

On the other hand, short cycle life due to internal short circuit is the most critical disadvantage of the zinc-based batteries. In the conventional batteries, since molecular diffusion is the only driving force of mass transfer in electrolyte, a thick concentration boundary layer of zinc (zincate) ion is formed near anode surfaces on charging and the system becomes far from equilibrium [1]. As a result, non-uniform dendritic electrodeposition of zinc occurs [2] that leads to battery short circuits. Choi et al. explained the mechanism of non-uniform zinc deposition in static electrolyte rechargeable zinc cells using electro-osmotic force [3,4]. Making use of flowing electrolyte is known as a method to suppress this influence by changing the mass transfer from diffusion control to convection control [5–13]. We have carried out experiments in flow-assisted zinc–nickel oxide batteries, and clarified the effects of flowing electrolyte on zinc morphology and battery performance [13]. We concluded that flowing electrolyte contributes to the modification of zinc morphology and can extend the battery cycle life significantly. More than 1500 cycles have been obtained while keeping the Coulombic efficiency at or above 90% by utilizing a deep-discharge reconditioning step every 15 cycles [13].

Loss of Coulombic efficiency during extended cycling is attributed to remaining zinc on anodes on discharge, hydrogen and oxygen evolution occurring as parasitic reaction, and other reasons such as corrosion within the sintered nickel electrodes [14]. The extent of gas evolution is determined by the balance of thermodynamics and kinetics of the hydrogen and oxygen, and those of the main reduction–oxidation reactions in the battery. Regarding zinc–nickel oxide batteries, both hydrogen and oxygen are often evolved [15–21]. From a hazard point of view, hydrogen has the potential of ignition, and gas evolution itself gives rise to an internal pressure increase which can also lead to explosion in sealed batteries. From a maintenance point of view, gas evolution introduces additional complications, since water is consumed by the gas evolution if no recombination mechanism exists. Thus, gas management is an important challenge in battery development and a number of studies have carried out on gas evolution and its suppression. For example, Arkhangel'skaya et al. [15] have developed nickel oxide electrodes using spherical nickel hydroxide that absorb hydrogen and oxygen. However, past studies [15–21] have rarely discussed in such a way that how the evolved gas affects to the battery performance. For the suppression of hydrogen evolution, a wide variety of additives have proven effective [20–26]. However, most of the studies have just shown the effects of additives on hydrogen evolution potential and zinc morphology, and the real impacts in batteries have scarcely been discussed. Furthermore, even though a flowing

* Corresponding author at: Dept of Chemical Engineering, City College of New York, 140th St at Convent Ave, Steinman Hall #314, New York, NY 10031, USA. Tel.: +1 212 650 8136; fax: +1 212 650 6660.
E-mail address: yito@che.ccny.cuny.edu (Y. Ito).

0378-7753/$ – see front matter © 2011 Elsevier B.V. All rights reserved.
doi:10.1016/j.jpowsour.2011.03.025

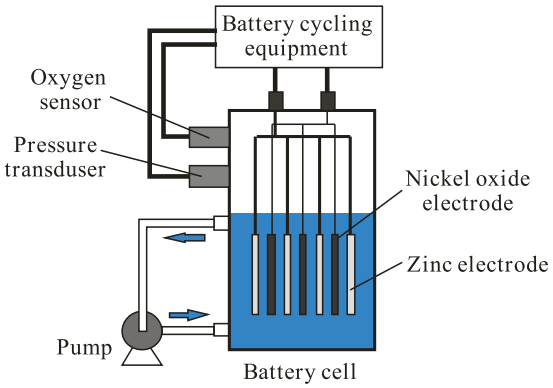

Fig. 1. Experimental apparatus.

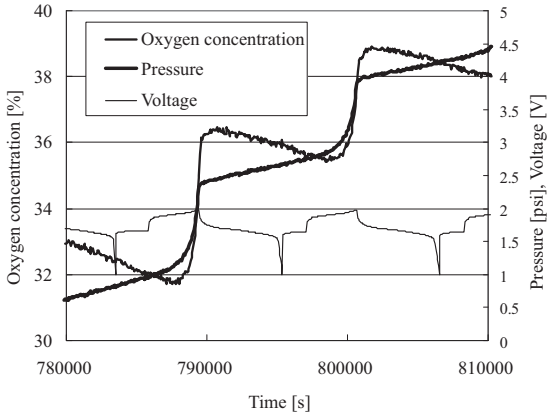

Fig. 2. Voltage, pressure, and oxygen concentration against time (the flowing case).

electrolyte is known to modify zinc morphology and the battery performance, its effects on gas evolution have not been well understood. To model and predict gas evolution in such flow-assisted batteries, it is essential to clarify the gas evolution quantitatively in a flow-assisted battery. Also, quantitative analysis of gas evolution essentially contributes to designing of batteries with a hydrogen and oxygen recombining system such as a catalytic recombiner [1], which is widely used for conventional batteries.

Therefore, we have conducted experiments on gas evolution in a sealed zinc–nickel oxide battery for with and without flow assisted cases. The effects of flowing electrolyte on gas evolution were quantitatively evaluated and the impacts on battery performances were discussed.

2. Experimental

Fig. 1 shows the schematic of the experimental apparatus. Metal zinc as negative (anode) electrode was deposited on polished nickel coated copper sheets serving as substrate. Sintered nickel oxide electrodes (Jiangsu Highstar Battery Manufacturing) were used as cathodes. The overall stoichiometry in the battery is as follows on discharge:

$$Zn + 2NiOOH + 2H_2O \Rightarrow Zn(OH)_2 + 2Ni(OH)_2$$

The test cell was a prismatic configuration and had a capacity of 2.2 Ah. The cell pack consisted of 3 positive and 4 negative plates alternately layered via spacers that have the thickness of 2.4 mm. Zinc oxide (Fisher Scientific ACS Grade) at a concentration of 60 g L^{-1} was initially dissolved into 45 wt% potassium hydroxide (KOH) solution (Fisher Scientific) as electrolyte. A KOH of relatively high concentration was used to maximize zincate solubility. The electrolyte flows from the bottom to the top of the cell at an average velocity of 3 mm s^{-1} in the flowing case. In the non-flowing case, the electrolyte was sufficiently circulated during the rest cycle before the charge cycle (after the discharge cycle) to avoid battery deterioration caused by dendritic growth of zinc, since the purpose of this study is to clarify the effects of flowing electrolyte on gas evolution. Evolved gases were accumulated in the head space of the cell. The concentration of the oxygen in the head space was measured by an oxygen sensor (Apogee SO-110). The internal pressure of the cell was measured by a pressure transducer (Measurement Specialties MSP300) which is also attached to the head space of the cell.

Galvanostatic battery cycling experiments were carried out for charge and discharge rates of 1 C and 0.5 C, respectively. Charge was terminated when a battery cell was fully charged to the full rated capacity of the sintered nickel oxide electrodes, and discharge was terminated when the cell voltage dropped to 1.0 V. Reconditioning was done every 5 cycles. This consisted of a deep-discharge at a 0.23 C rate to an end of discharge voltage of −0.2 V. All the data including the oxygen concentration and pressure were recorded to turnkey battery cycling equipment (Arbin Instruments BT-2000) every 60 s.

3. Results and discussion

3.1. Regular cycle

Fig. 2 shows an example of the time series of pressure and oxygen concentration in the cell for a few successive cycles. Partial oxygen pressure and the amount of oxygen evolved were calculated based on these data using ideal gas law. Assuming that the rest of the pressure increase is by hydrogen, the partial pressure and the amount of hydrogen evolved were calculated. It is confirmed by the preliminary experiments that the temperature fluctuation is negligibly small.

Fig. 3 shows the hydrogen evolution in Ah against time. The hydrogen on Ah basis was calculated from that on molar basis by Faraday's law. Hydrogen is evolved throughout the cycling. On charge, many studies have reported that hydrogen is evolved from zinc (anode) side [12,13,15,17]. Because of the formation of concentration boundary layer and the lower concentration of zinc (zincate) ion near the zinc anodes in the non-flowing case, hydrogen evolution tends to occur more instead of zinc electrodeposition.

On the other hand, on discharge, hydrogen can theoretically be evolved from the cathode (nickel oxide). However, from a thermodynamic point of view, hydrogen evolution should not start until the cell voltage drops much lower, near 0 V. Other possibilities are zinc corrosion and that hydrogen evolved on charging is released from voids within the zinc electrodeposit during discharging. Fig. 4 shows the time elapsed images of the zinc anode in a cycle. The

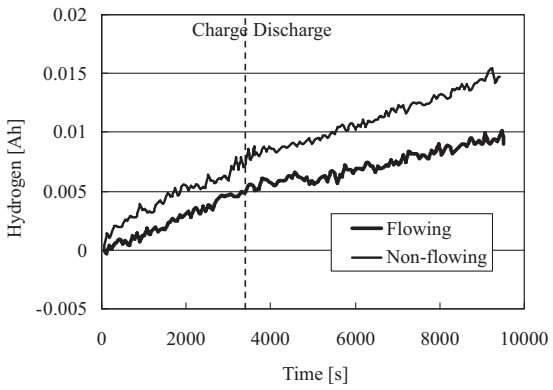

Fig. 3. Hydrogen evolution against time.

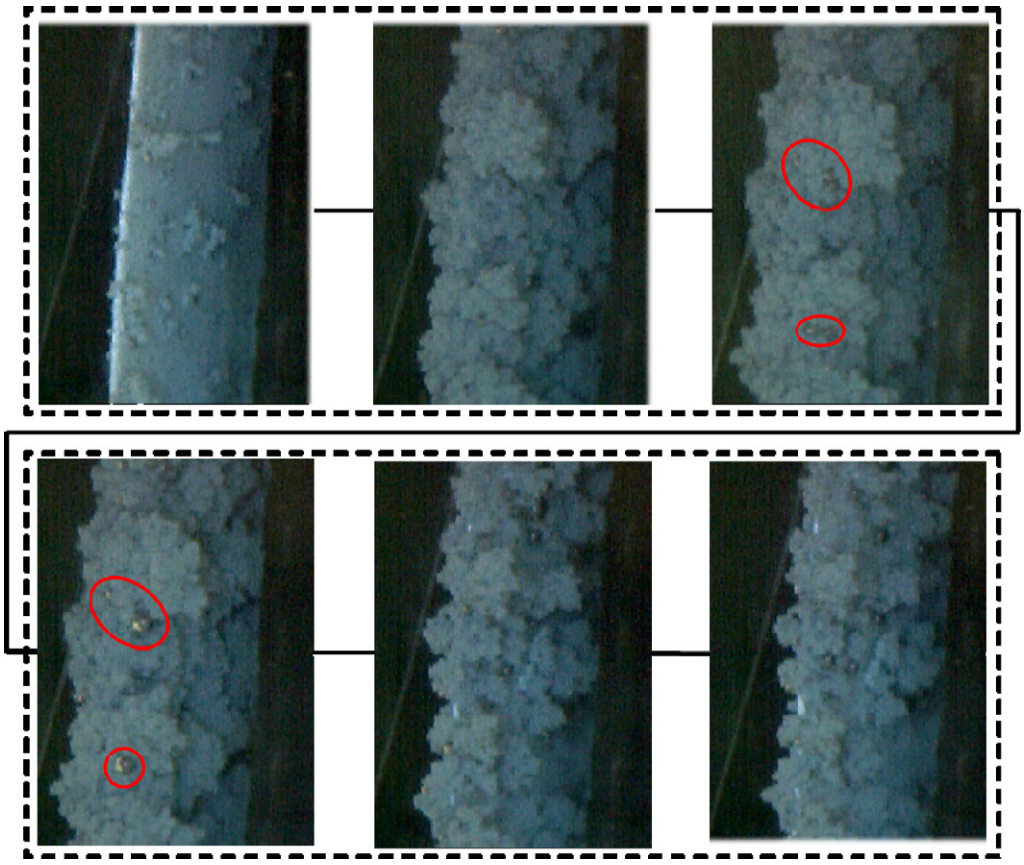

Fig. 4. Electrodeposition of zinc.

upper images are on charging and the lower images are on discharging. As indicated by circles in Fig. 6, the evolved bubbles on charging, which are presumed to be hydrogen, do not detach from the surface on charging and detach on discharging. Also, there are quite a few bubbles that appear as zinc dissolves on discharging. From a thermodynamic point of view, these bubbles should not be oxygen and, in fact, oxygen in the cell does not increase on discharging. Therefore, these are expected to be hydrogen which is generated on charging. Considering zinc morphology is mossy and porous, it is quite possible that hydrogen is contained within the voids of the zinc on charging. Thus, although it is impossible to determine when these bubbles appearing on the anodes on discharging were generated, the increase of the hydrogen on discharging is probably the hydrogen evolved on charging and they exposed and released as the zinc dissolves into the electrolyte on discharging.

Fig. 5 shows oxygen evolution in Ah against time. Oxygen is drastically evolved toward the end of charge for both the cases. This oxygen evolution is from the positive (nickel oxide) electrodes and this phenomenon in zinc–nickel oxide batteries has been reported in many previous works. [15,17,18] The figure also shows that oxygen is evolved more in the non-flowing case than the flowing case. Though we did not compare the differences of crystal structure of the nickel oxide electrodes between the flowing and non-flowing cases, considering that oxygen evolution basically occurs on overcharging, and that electrolyte (KOH) concentrations affect the performance of sintered nickel oxide electrodes [27], oxygen evolution tends to occur more than the reaction between nickel oxide and hydroxide ion in the non-flowing case, because of the concentration gradient of the hydroxide ion at the electrodes surfaces. On discharging, oxygen is not evolved for both the cases, and the curves rather show a tendency of slight decrease of oxygen in the cell. This indicates that oxygen is slightly recombined on discharging, probably by the reduction on the positive plates. Though the oxygen concentration in the electrolyte was not measured in this study, considering the solubility of oxygen in the 45% KOH is only about 2×10^{-3} Ah L^{-1} [28], it is not caused by the dissolution into the electrolyte. This trend was observed during the rest cycle too. Quantitatively, the amount of the evolved oxygen on an Ah basis is about five times as much as that of hydrogen for both the cases.

Fig. 6 shows the charge–discharge curves against time that corresponds to Figs. 3 and 5. The overpotential on charging in the non-flowing case is higher than that in flowing case. For the non-flowing case, the end of charging voltage was 2.06 V, whereas that for the flowing case was 1.98 V. On discharging, the curves for both the cases are almost identical, but the flowing case discharged a little more than the non-flowing case.

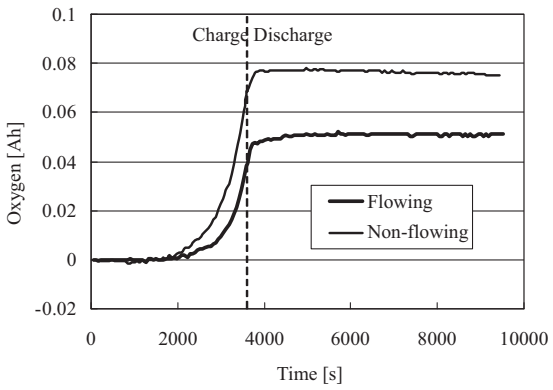

Fig. 5. Oxygen evolution against time.

Table 1
Coulombic and energy efficiencies.

	Charge capacity [Ah]	Discharge capacity [Ahl	Charge energy [Wh]	Discharge energy [Wh]	Coulombic efficiency [%]	Energy efficiency [%]
Flowing	2.2	2.11	4.2	3.50	96.1	83.5
Non-flowing	2.2	2.07	4.35	3.39	94.1	78.1

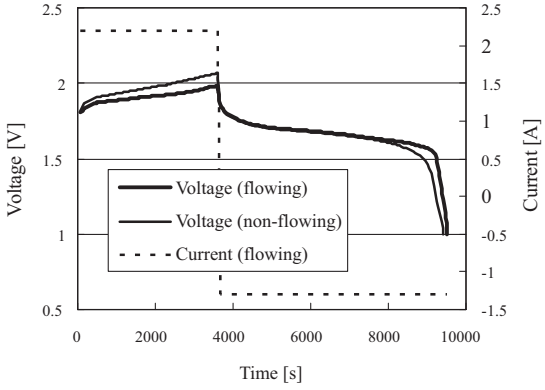

Fig. 6. Charge–discharge curve.

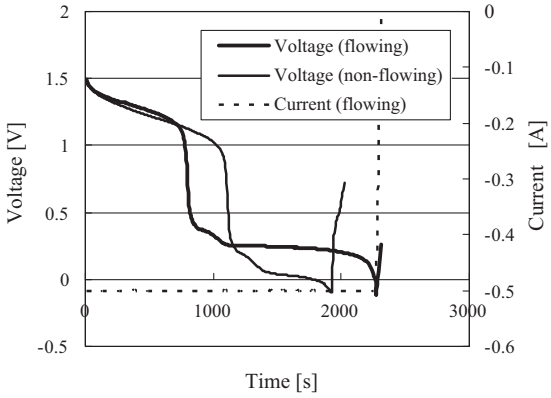

Fig. 7. Voltage curve (reconditioning cycle)

The roundtrip Coulombic and energy efficiencies are shown in Table 1, together with the charge and discharge capacities and energies. As shown, both the Coulombic and energy efficiency in the flowing case were higher than those in the non-flowing case.

The fractions of hydrogen and oxygen evolutions against the cell capacity and Coulombic loss per cycle are summarized in Table 2. For both the cases, the fractions of hydrogen and oxygen evolution against the cell capacity for the flowing case are 0.45% and 2.32%, respectively, whereas those in the non-flowing case are 0.66% and 3.45%, respectively. On the other hand, against Coulombic loss, those are about 11% and 60%, respectively for both the cases. These results suggest that the cell Coulombic efficiency mainly depends on the nickel oxide electrode in the battery.

3.2. Reconditioning cycle

As mentioned above, in a zinc–nickel oxide cell, the zinc electrode typically is more Coulombically efficient than the nickel oxide electrode. Thus, a discharge reserve of zinc will progressively be generated with cycling absent some means of oxygen recombination on the anode or a periodically applied stripping procedure. This generation of a zinc discharge reserve can also accelerate the non-uniform electrodeposition of zinc which can lead to the reduction of discharge capacity. Therefore, we have found it beneficial to periodically recondition the zinc anodes. The reconditioning procedure consisted of a slow discharge to a lower voltage [13].

Figs. 7 and 8 show the voltage curve and hydrogen evolution in Ah against time, respectively. The data in the rest cycling following the discharge cycle is also shown in Fig. 8, since hydrogen is continuously evolved. Oxygen evolution behavior was the same as the regular discharging for both the cases. It is found from Fig. 7 that the voltage curve has two stages; a gentle to steep drop (Stage 1), and a plateau to steep drop (Stage 2). This is caused by the different electrochemical reaction occurring on the cathode side, whereas the reaction on the anode side is zinc dissolution at both the stages. At the Stage 1, remained nickel oxyhydroxide is electrochemically reduced to nickel hydroxide, as in the regular discharge. Once the nickel oxyhydroxide was completely reduced, hydrogen starts to be evolved instead until zinc remained on the anode side almost completely dissolves into the electrolyte. In fact, rapid hydrogen evolution clearly begins in Fig. 8, when the voltage plateau begins in Fig. 7. Since the nickel oxide electrodes in the non-flowing case do not perform as efficiently as that in the flowing case on regular cycling, the Stage 1 lasts longer in non-flowing case. On the contrary, the discharge at the Stage 2 in the flowing case is longer than that in the non-flowing case. This behavior of the Stage 2 can depend on several factors such as residual zinc on the anode surfaces, performances of both the electrodes on regular cycles, and the amount of zinc taken out by the Stage 1. One of the reasons of this longer Stage 2 in the flowing case is the lower resistance due to the lower concentration of zinc (zincate) ion near the zinc anodes in the flowing case. As a result, reconditioning cycle worked more effectively in the flowing case. In accordance with this phenomenon, the amount of hydrogen evolved in the flowing case is larger than that in the non-flowing case. Since zinc which does not discharge in the past regular cycles discharges on the reconditioning cycle, the overall Coulombic efficiency includ-

Table 2
The fraction of gas evolution against the cell capacity and Coulombic loss.

	Cell capacity [%]		Coulombic loss [%]	
	H_2	0_2	H_2	0_2
Flowing	0.45	2.32	11.4	59.5
Non-flowing	0.66	3.45	11.2	58.5

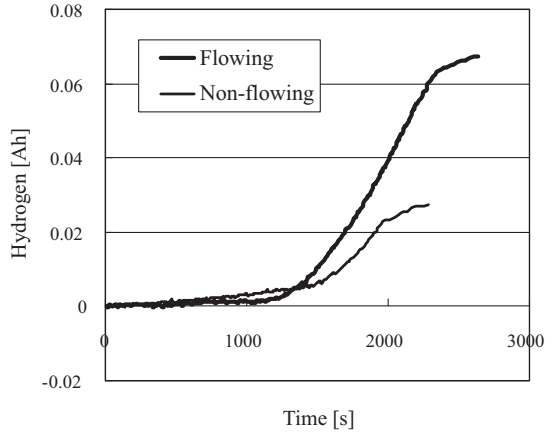

Fig. 8. Hydrogen evolution against time (reconditioning cycle).

Table 3
Coulombic efficiency including reconditioning cycle.

	Regular cycle [%]	Reconditioning cycle [%]	Total [%]
Flowing	95.9	14.1	110.0
Non-flowing	93.7	12.3	106.0

ing reconditioning cycle becomes more than 100%, as shown in Table 3.

4. Conclusions

An experimental study on gas evolution in a sealed zinc–nickel oxide cell was carried out for with and without flow-assisted cases. The main remarks obtained are summarized as follows:

- Both hydrogen and oxygen evolution are suppressed by making the electrolyte flowing on the regular cycle. This is due to the increased cell polarization in the non-flowing case caused by the concentration boundary layer of zinc (zincate) ion near the anode surfaces.
- The fraction of Coulombic loss attributed to gas evolution is about 70% in the flowing case, whereas it is about 30% in the non-flowing case. This amounts to less than 5% of cell capacity for both the cases.
- More hydrogen is evolved in the flowing case than in the non-flowing case during the reconditioning cycle.

These obtained results are believed to significantly contribute to the designing and modeling of zinc–nickel oxide batteries.

Acknowledgements

This work was performed under grants from the New York State Foundation for Science (NYSTAR, #C040067), Advanced Research Project Agency–Energy (ARPA-E, #DE-AR0000150), and National Energy Technology Laboratory (NETL, #DE-EE0004224).

References

[1] K. Fukami, S. Nakanishi, H. Yamasaki, T. Tada, K. Sonoda, N. Kamikawa, N. Tsuji, H. Sakaguchi, Y. Nakato, J. Phys. Chem. C 111 (2007) 1150.
[2] D. Linden, T.B. Reddy (Eds.), Handbook of Batteries, third ed., 2001.
[3] K.W. Choi, D.N. Bennion, J. Newman, J. Electrochem. Soc. 123 (1976) 1616.
[4] K.W. Choi, D.N. Bennion, J. Newman, J. Electrochem. Soc. 123 (1976) 1628.
[5] R.D. Naybour, J. Electrochem. Soc. 116 (1969) 520.
[6] D.P. Sutija, R.H. Muller, C.W. Tobias, J. Electrochem. Soc. 141 (1994) 1477.
[7] J. Jorne, M.G. Lee, J. Electrochem. Soc. 143 (1996) 865.
[8] R.Y. Wang, D.W. Kirk, G.X. Zhang, J. Electrochem. Soc. 153 (2006) C357.
[9] R. Frank, McLarnon, J. Elton, J. Cairns, Electrochem. Soc. 138 (2) (1991).
[10] R.G.A. Wills, J. Collins, D. Stratton-Campbell, T.J. Low, D. Pletcher, F.C. Walsh, J. Appl. Electrochem. 40 (2010) 955.
[11] J. Cheng, L. Zhang, Y.S. Yang, Electrochem. Commun. 9 (2007) 2639.
[12] L. Zhang, J. Cheng, Y.S. Yang, J. Power Sources 179 (2008) 381.
[13] Y. Ito, M. Nyce, R. Plivelich, M. Klein, D. Steingart, S. Banerjee, J. Power Sources 196 (2011) 2340.
[14] M. Oshitani, T. Takayama, K. Takashima, S. Tsuji, J. Appl. Electrochem. 16 (1986) 403.
[15] Z.P. Arkhangel'skaya, M.M. Loginova, T.B. Kas'yan, D.A. Vinogradova, Rus. J. Appl. Chem. 77 (2004) 67.
[16] P.-C. Hsu, S.-K. Seol, T.-N. Lo, C.-J. Liu, C.-L. Wang, C.-S. Lin, Y. Hwu, C.H. Chen, L.-W. Chang, J. J.H., G. Margaritondoi, J. Electrochem. Soc. 155 (2008) D400.
[17] C. Cha, J. Yu, J. Zhang, J. Power Sources 129 (2004) 347.
[18] P.H.L. Notten, E. Verbitskiy, W.S. Kruijt, H.J. Bergveld, J. Electrochem. Soc. 152 (2005) A1423.
[19] N.D. Nikolicˇ, G. Brankovicˇ, M.G. Pavlovicˇ, K.I. Popov, J. Electroanal. Chem. 621 (2008) 13.
[20] J.L. Zhu, Y.H. Zhou, C.Q. Gao, J. Power Sources 72 (1998) 231.
[21] M.F. de Carvalho, W. Rubin, I.A. Carlos, J. Appl. Electrochem. 40 (2010) 1625.
[22] Y.–H. Wena, J. Chenga, S.–Q. Ning, Y.-S. Yanga, J. Power Sources 188 (2009) 301.
[23] C.W. Lee, K. Sathiyanarayanan, S.W. Eoma, H.S. Kima, M.S. Yun, J. Power Sources 159 (2006) 1474.
[24] M.I. da Silva Pereira, Electrochim. Acta 52 (2006) 863.
[25] Y.-H. Wen, J. Cheng, L. Zhang, X. Yan, Y.-S. Yanga, J. Power Sources 193 (2009) 890.
[26] C.W. Lee, K. Sathiyanarayanan, S.W. Eoma, H.S. Kima, M.S. Yun, J. Power Sources 160 (2006) 161.
[27] H. Vaidyanathan, K. Robbins, G.M. Rao, J. Power Sources 63 (1996) 7.
[28] K.E. Gubbins, R.D Walker Jr., J. Electrochem. Soc. 112 (1965) 469.